ARTICLE

Recent Advances in Surface Modified Gold Nanorods and Their Improved Sensing Performance

Received 00th January 20xx,
Accepted 00th January 20xx

DOI: 10.1039/x0xx00000x

Ying Bao* and Ayomide Oluwafemi

Gold nanorods (AuNRs) have received tremendous attention recently in the fields of sensing and detection applications due to their unique characteristics of surface plasmon resonance. Surface modification of the AuNRs is a necessary path to effectively utilize their properties for those applications. In this Article, we have focused both on demonstrating the recent advances on methods of surface functionalization of AuNRs as well as their use for improved sensing performance using various techniques. Main surface modification methods discussed include ligand exchange with the assists of thiol-group, layer by layer assembly method, and depositing inorganic materials with desired surface and morphology. Covered techniques that can then be used for using those functionalized AuNRs include colourimetric sensing, refractive index sensing and surface enhance Raman scatttering sensing. Finally, the outlook on the future development of surface modified AuNRs for improved sensing performance is considered.

Introduction

Over the past few decades, noble metal nanoparticles have shown great promise for their use in many areas such as sensing, imaging, catalysis, and biomedicine, due to their distinct physical and chemical properties, which cannot be found in their bulk counterparts. This is because in the nanoscale region (~100 nm), these metal particles' electronic, optical, and catalytic properties have dramatic changes due to their large surface area-to-volume ratio and space confinement of the free electrons.[1] A key example is that an external light illumination can excite the free electrons in these nanoparticles to have collective oscillation and when the frequency of the external light matches the inherent frequency of the free electrons, a localized plasmon resonance (LSPR) will be formed.[2] The LSPR can cause significant enhancement of the electromagnetic field at and near the surface of these nanoparticles, which is a crucial feature for detection, plasmonic enhanced spectroscopy and other applications. The plasmon resonance position can be characterized by using an UV-visible spectrophotometer and, when doing so, a plasmon band (extinction peak) will be observed with high extinction coefficient (up to 10^{11} M^{-1} cm^{-1}).[3]

Such LSPR frequency is strongly dependent on the type of particle material, morphology, and surrounding environment.[4-6] By optimizing the synthesis condition, the LSPR frequency can be tuned to the ideal location in the spectral range for the requirements of specific applications. For spherical metal nanoparticles, the LSPRs are isotropic which gives poor adjustability and are only located in visible range due to the symmetric structure. On the other hand, non-spherical metal nanoparticles exhibit anisotropic optical and electronic responses. Among the various anisotropic morphologies of gold nanoparticles, gold nanoparticles with an elongated rod shape, gold nanorods (AuNRs), have gained the most popularity. Due to their anisotropic structures, AuNRs possess two characteristic plasmon bands: a transverse band and a longitudinal band. The transverse band is often located between 520-540 nm in the visible region while the longitudinal band can be tuned to a wide spectral range, from visible to near-infrared (NIR) region (over 1000+ nm), by tailoring the aspect ratio of the AuNRs -- the ratio between length and width. As shown in Figure 1, with the increased aspect ratio of the AuNRs, (Figure 1a) the colour of the solution and the peak of the longitudinal band has shifted dramatically (Figure 1b-c).[7] This optical behaviour responsible for these effects has been well understood via Gans theory.[8] The high sensitivity of the longitudinal band to its morphology and surrounding environment allows AuNRs to be excellent candidates for applications in refractive index and colorimetric based sensing strategies.

Another principal effect that makes AuNRs great candidates for sensing or detection applications is surface enhanced Raman scattering (SERS). At a more basic level, Raman scattering is an inelastic scattering of photons by molecules which are excited to higher vibrational or rotational energy levels, providing a useful molecular fingerprint of materials.[9] Unfortunately, the Raman signal of molecules is weak which requires a high concentration of molecules to obtain a reasonable Raman spectrum. However, if the target molecules are on or near the surface of metal nanomaterial, the Raman signal can be significantly enhanced by several orders of magnitude due to the surface electromagnetic (EM) enhancement effects and this phenomenon is known as SERS.[10] AuNRs exhibit huge EM enhancement under resonated excitation, mainly at the ends of the rod, which decays exponentially as the distance from the surface increases, and the EM field can be further increased using AuNR assemblies or aggregates due to plasmon coupling. Furthermore, it is important to note that, due to the tuneable band in the NIR region, AuNRs are particularly suited for in-vivo

[a] *Department of Chemistry, Western Washington University, Bellingham, Washington, 98225, USA. E-mail: Ying.Bao@wwu.edu;*

sensing applications because 1) the rate of absorption of NIR radiation by the living tissue is very small, thus allowing the optimal light penetration; 2) NIR light is less likely to excite background fluorescence.

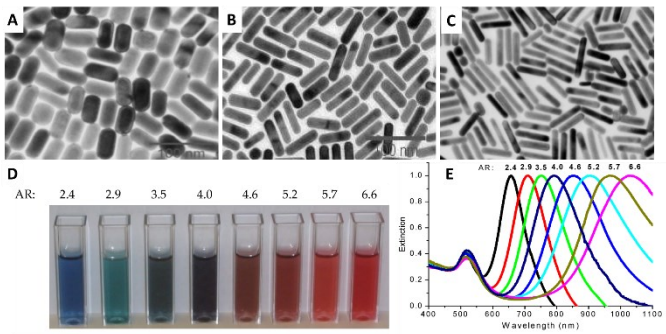

Figure 1: Tuneable optical properties of AuNRs by changing the aspect ratios (AR).[7] (A–C) TEM images of AuNRs with AR of 2.9 (A), 4.0 (B), and 4.6 (C); The solution colour of AuNRs with various ARs (D) and their different SPR wavelength (E). Reproduced with permission from ref. 7. Copyright 2022, Multidisciplinary Digital Publishing Institute.

Until now, various methods have been developed to produce AuNRs with different structures. Wet chemistry-based approaches include seed mediated growth methods, electrochemistry methods, and template methods. Synthesis and growth mechanisms for AuNRs using various methods have been well summarized in recent reviews and will not be discussed further here.[11-14] With the synthesized AuNRs, surface modification becomes a critical step to nearly all applications of AuNRs. Numerous strategies layer by layer method,[15] ligand exchange,[16] silica coating,[17] and covalently linking,[18] etc. have been developed and employed to tune the NR surface chemistry with various materials ranging from polyelectrolytes, mesoporous silica and thiol molecules to protein, bio-functional molecules, other inorganic/organic materials, which allow the success on their wider applications in sensing, electronics, drug delivery, biological therapy, etc..

In this article, we highlight on summarizing recent advances (since 2012) on the surface functionalization of AuNRs and their use in improved sensing performance.

Surface functionalization of AuNRs for sensing

As mentioned above, without further effective surface functionalization, as-synthesized AuNRs are often not particularly useful for most applications, including sensing. For example, the most popular type of AuNRs are synthesized by a seed mediated approach in the presence of surfactant, such as cetyltrimethylammonium bromide (CTAB), cetyltrimethylammonium chloride (CTAC) or benzyldimethyl ammonium chloride (BDAC). CTAB is the most popular surfactant and is important to the synthesis of AuNRs because it acts not only as a structure directing agent to control the final nanorod shape, but also as stabilizer to prevent the as-synthesized AuNRs from aggregating. However, the CTAB surfactant appears to have several disadvantages for applications. First, CTAB is only stable in aqueous solutions with a lower pH value. Thus, situations such as high pH, high salt content or an organic solvent jeopardizes the stability of CTAB-coated AuNRs, thus limiting their application. Second, free CTAB molecules are cytotoxic to human cells, posing a problem for in vitro studies. Finally, the presence of CTAB surfactant can interfere with sensing processes by impacting AuNRs selectivity and sensitivity. These issues can be addressed via surface modification of the AuNRs with proper organic or inorganic materials, allowing for enhanced applications.

In this section, we will focus on summarizing recent progress in developing surface modification methods used to improve sensing applications for AuNRs.

2.1 Ligand exchange method

Since the metal-sulfur bond is known to be an exceptionally strong bond compared to other general functional groups, using thiol-ended molecule ligands is the most common approach to directly replace CTAB on the surface of AuNR through covalent attachment. Thiolated poly(ethylene glycol) molecules (PEG-thiol molecules) are one of most popular ligands for surface modification due to advantages such as high stability in various solvents and biocompatibility.[19-22]

For sensing applications, replacing the CTAB bilayer with a single layered PEGylated ligand will also reduce the steric hinderance, which will facilitate the analytes' interaction with the AuNRs for improved sensitivity.[23] For example, our group has directly mixed PEG-thiol molecules with a solution of CTAB coated AuNRs; this procedure is shown in Figure 2a. With sufficient mixture and ligand interaction, the PEG modified AuNRs were obtained after several rounds of purification, including multiple rounds of centrifugation and removal of the supernatant. Comparing the ^{1}HNMR spectrum of CTAB@AuNRs (some results are shown in Figure 2b), it is clear that the ^{1}HNMR spectrum of PEG@AuNRs, after the ligand-exchange process, shows significant decrease of the CTAB methyl resonance at 0.85 ppm (red dashed circle), and furthermore the presence of PEG long chain resonance at 3.5 ppm is clearly distinguishable. The PEG-thiol modified AuNRs were then used for mercury ion sensing which showed improved stability, sensitivity and selectivity compared to AuNRs that did not have the CTAB replaced.[24]

The thiolated PEG linkers are relatively large, which leads to relatively low surface-binding density. This gives the possibility of functionalizing additional different molecules on the surface of the AuNRs which might not be achievable without the thiolated PEG linkers contributing stability, resulting in a more targeted sensor.[25-26] For example, Priyadarshni and others have developed a sensor by stepwise chemical conjugation of AuNRs with mPEG-SH followed by meso-2,3-dimercaptosuccinic acid (DMSA), shown in Figure 2c. PEG, being hydrophilic in nature, was used to impart stability to the AuNR sensor in aqueous medium. The unbound -SH groups of DMSA were used to bind with arsenic species during analysis. Due to the ion-induced aggregation of AuNRs through an arsenic complex, such sensors can selectively detect both As^{III} and As^{V} ions with a detection limit of ~1.0 ppb.[26] This strategy is also used to modify AuNRs

with biofunctional molecules. Yasun et al. modified AuNRs with PEG ligands and a 15-mer thrombin aptamer for protein detection. The PEG ligand was used to stabilize the AuNR while the aptamer was used to capture the targeted protein for detection.[25]

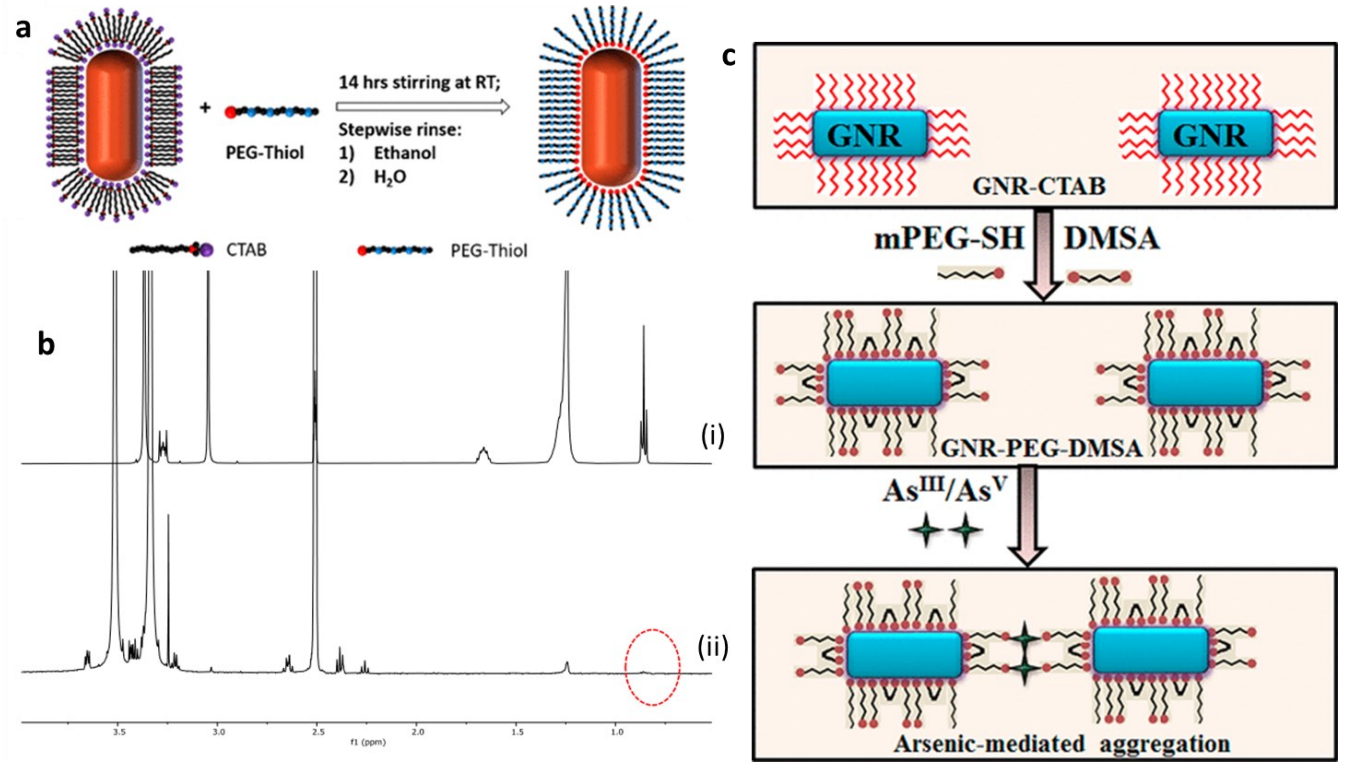

Figure 2: (a) Schematic illustration of the ligand-exchange process between PEG-thiol ligands and CTAB ligands on the surface of AuNRs.(b) 1H NMR spectra of (i) CTAB@AuNR, (ii) PEG@AuNR.[24] (c) Schematic of fabrication of AuNR sensor, GNR-PEG-DMSA and its interaction with arsenic ions (As^{III}/As^{V}) in water. [25] Reprinted with permission from ref. 24, 25. Copyright 2021 and 2012, American Chemical Society.

When using ligand exchanges to improve AuNRs for biosensing applications, various alternatives to binding co-ligands via CTAB replacement on the nanorod surface include attaching thiolated PEG linkers with certain functional groups (e.g. carboxyl and amino group) or adding small thiol-terminated molecules (e.g. 11-mercaptoundecanoic acid (MUA), cysteamine) or thioctic acids (e.g. disulfide, Cyclic disulfides) to the AuNR surfaces.[27] While surface modification using these approaches is known to be relatively difficult, developing effective strategies for the exchange of CTAB on the surface of AuNRs with MUA,[28-29] peptidic ligands,[30] and others[31-32] has been an area of active research in recent years.

2.2 Layer-by-layer method

The layer-by-layer (LbL) method of surface modification is to sequentially deposit negative and positive charged polyelectrolytes on the charged surface of the AuNRs to manipulate their surface properties. The successful deposition of the polyelectrolytes can be confirmed with zeta potential (effective surface charge) measurement.[33-34] This method can improve the stability and biocompatibility of AuNRs, as well as sensing performance. Singamameni group has used the LbL method to modify the AuNRs with various charges, which were used to effectively adsorb analytes of interests.[35-36] For example, they used polystyrenesulfonate (PSS) and poly(diallyldimethylammonium chloride) (PAH) functionalized AuNRs via the LbL method which can then effectively capture their opposite charged analytes. The varying responses of the Raman spectra due to the diverse chemical functionalizations of the AuNRs, were collected, allowing them to not only recognize the components of the mixtures but also quantify the mixing ratio.[35]

Furthermore, these polyelectrolytes can also adsorb antibodies, proteins, dyes or other targeted molecules via non-covalent interaction.[37-38] Thus, the final charged surface can also be used for subsequent chemistry which opens additional routes for sensing applications. For example, polyacrylic acid (PAA) coated AuNRs terminate with a carboxylic acid group which can be covalently conjugated with amine terminated biotin or biomolecules via the 1-ethyl-3-(3-(dimethylamino)propyl)-carbodiimide (EDC)-mediated coupling reaction which can be used for biosensing including streptavidin-biotin binding, or antibody-antigen associations.[39-40]

The LbL method can also control the thickness around the AuNRs which determines the refractive index of the AuNRs' surrounding environment, and is thus a crucial parameter affecting the LSPR response and sensitivity.[41-42] Tian and co-workers investigated the influence of the dimension of AuNRs on their distance-dependent LSPR sensitivity and EM decay length using the LBL method. PSS and PAH were used to

alternatively deposit with the desired number of bilayers to control the thickness. From the AFM results of AuNRs with 10 bilayers deposition, it is clearly shown that the LBL deposition results in a linear increase of film thickness as well as a conformal deposition which essentially did not change the diameter of AuNRs. The extinction spectra after each bilayer deposition reveals a progressive red-shift in the LSPR wavelength and a monotonic increase in LSPR intensity due to the increase in the refractive index (from air to polymer layer). In addition, the incremental LSPR shift decreased with the addition of polyelectrolyte layers, indicating that LSPR sensitivity of AuNR decreases with the increase in the distance from the AuNR surface. For EM decay length, they found that it increases linearly with both nanorod length and diameter, although to variable degrees. They showed that the LbL method is able to precisely control the EM decay length of nanostructures, enabling the rational selection of plasmonic nanotransducer dimensions for particular biosensing applications.[42] Urrutia et al. enveloped AuNRs in thin film created via the LbL technique for applications in optical fiber sensing. The film thickness greatly impacted the plasmonic bands' response and they found that the thicker polymer/AuNRs overlays generated a new lossy mode resonance (LMR) band which is more sensitive than LSPR modes. Under various relative humidities, the LMR band showed sensitive displacement while the LSPR modes were stable. Such features allows AuNR/film sensor to have excellent sensitivity with the possibility of optimization and opening the door to other new sensing applications.[41]

2.3. Surface coating method using inorganic materials

2.3.1 AuNR-silica nanostructures

This surface coating method refers to depositing inorganic materials on the surface of AuNRs. Mesoporous silica is the most commonly used coating material in the sensor field due to its biosafety, straightforward synthesis process and ability to enhance the stability of AuNRs. The Stöber method[43-44], first used for synthesizing SiO_2 spheres, has been adapted for overcoating AuNRs with SiO_2, with a relatively simple single step method developed to deposit silica on CTAB-capped AuNRs.[17] In this process, a solution of CTAB coated AuNRs dispersed in water is first adjusted to pH = 10-11 by NaOH or ammonium hydroxide. A solution of tetraethylorthosilicate (TEOS) in an alcohol (methanol or ethanol) is then injected into the AuNR solution under gentle stirring. The CTAB molecules adsorbed on the surface of AuNR act as templates for the deposition of the hydrolyzed TEOS species onto the AuNRs. The resulting silica shell exhibits a mesostructure with disordered pores around 4 nm in diameter. The mesostructured nature of silica on the surface of AuNR can act as a SERS platform with a built-in sieve to limit the size of objects that can reach the AuNR surface.[45] In a recent study, Haynes and co-workers demonstrated that mesoporous silica coated AuNRs can be used as this type of suspension-phase SERS sensing platform with a built-in analyte size cutoff. Their work generally shows that the transport of molecules through silica mesopores is highly dependent on the size of the molecule, and specifically that mesoporous silica coated AuNRs with pores of ~4 nm diameter are able to sense analytes with molecular dimensions smaller than 1.5 nm.[46] The same group also studied how SERS performance is impacted by factors including adsorbed molecules, attributes of the silica shell, as well as the solvent media. They found that the SERS signal intensities from hydrophobic analytes are enhanced when the pore size, hydrophobicity of the shell, and ionic strength are increased. The existing silica shell facilitates efficient adsorption of the analyte to the gold core and enhanced sensitivity to environmental refractive index changes.[47]

The porosity, thickness, and morphology of the silica shell can be finely controlled by varying the synthesis conditions[48-52] which can be used to optimize their desired sensing performance.[53-54] In a recent study, Boujday and co-workers coated AuNRs with a silica shell based on dissociation of TEOS hydrolysis and condensation reactions. Through this strategy, they were able to create AuNRs each coated with a thick silica shell that had an organized mesoporosity, aligned either in parallel or perpendicular to the AuNR surface. In addition, ultrathin and homogeneous silica shells (AuNR@t-SiO2) of controllable thickness in the range 2–6 nm were produced when using mercaptopropyltrimethoxysilane as a surface primer prior to TEOS condensation.[53] The three protocols are shown in scheme 1. The ultrathin silica shell-coated AuNRs showed a 30% higher refractive index sensitivity factor than that of CTAB-capped AuNRs, indicating a promising potential for the development of LSPR biosensors.

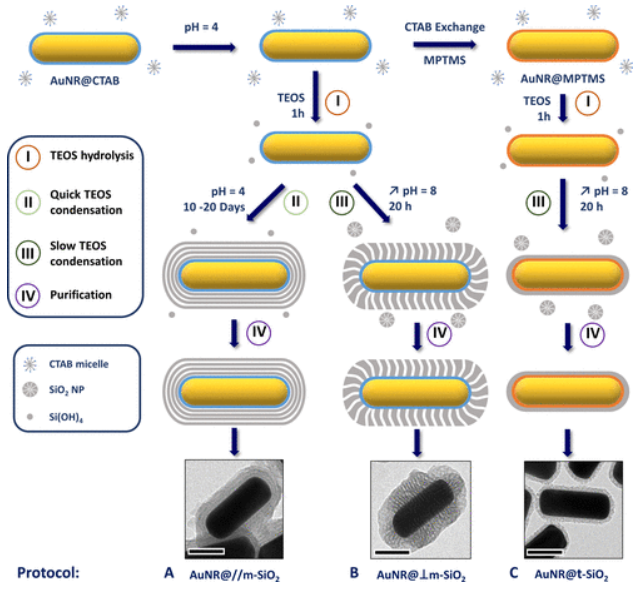

Schematic 1: Scheme 1. Pathways Adopted for the Three Protocols Developed to Grow a Silica Shell on AuNRs: (A) AuNR@//m-SiO_2, (B) AuNR@⊥m-SiO_2, and (C) AuNR@t-SiO_2.[53] Reprinted with permission from ref. 53. Copyright 2021, American Chemical Society.

Our group and others also have found that under certain experimental conditions, the silica shell grows exclusively or mostly on the two tips of the nanorods, leading to dumbbell/peanut-shaped coating, which can be either desired or undesired, depending on the objective.[52, 55-57] From our study, we believe that dumbbell-shaped particles are formed

because of the energy barrier that TEOS needs to cross to access the hydrophobic space located in the middle of the CTAB double layer surrounding the AuNRs. This energy barrier is stronger on the sides of the AuNRs than on the tips, leading to a favourable nucleation of the silica coating around AuNR tips, and varies with the composition of the reaction medium (concentration of TEOS, CTAB, and ethanol); see Figure 3 a-c. The dumbbell shaped particles show significantly higher SERS intensity than the fully coated AuNRs, which is understandable since the average thickness of the silica shell for dumbbell morphology was much smaller.[55] Murphy group fabricated similar dumbbell structures with mesoporous silica on the tips of AuNRs. In their work, they took advantage of anionic charged mesoporous silica, which enabled surface-enhanced Raman scattering (SERS) detection of the cationic dye methylene blue at lower concentrations than observed when silica coated the entire rod.[46]

2.3.2 AuNR-metal/metal oxide nanostructures

Depositing a second metal such as Ag, Pd, or Pt on the surface of AuNRs, in addition to silica, for improved sensing applications has received much attention.[58-59] The seed-mediated growth method is often chosen to fabricate a secondary metal shell on the surface of pre-grown AuNRs with different morphologies due to the ability to control the size, shape and composition of the shell. Reaction conditions such as pH, temperature, and reducing agent are determining factors on the resulting morphology.[60-65]

Among those metals, Ag is the most used since its nanocrystals exhibit much weaker plasmon damping and feature larger light scattering compared to nanocrystals made of other metals. With silver deposition, the nanostructure potentially gains an additional benefit called a "plasmonic focusing" effect, resulting in a stronger reduction of the ensemble plasmon linewidth and implying a long plasmon lifetime, a large field enhancement, as well as a high sensing sensitivity.[62] In a recent study, Chen and co-workers prepared a Ag shell on Au nanorods by reducing silver ions by ascorbic acid in the presence of PVP and CTAB mixture, which then were used to detect microRNA141 (miR-141). As illustrated in Figure 3d, amplification cascades with catalysed hairpin assembly (CHA) and hybridization chain reactions (HCR) were triggered in response to miR-141 to produce catalytic hemin/G-quadruplex HRP-mimicking DNAzymes for the degradation of H_2O_2 into hydroxyl radicals.

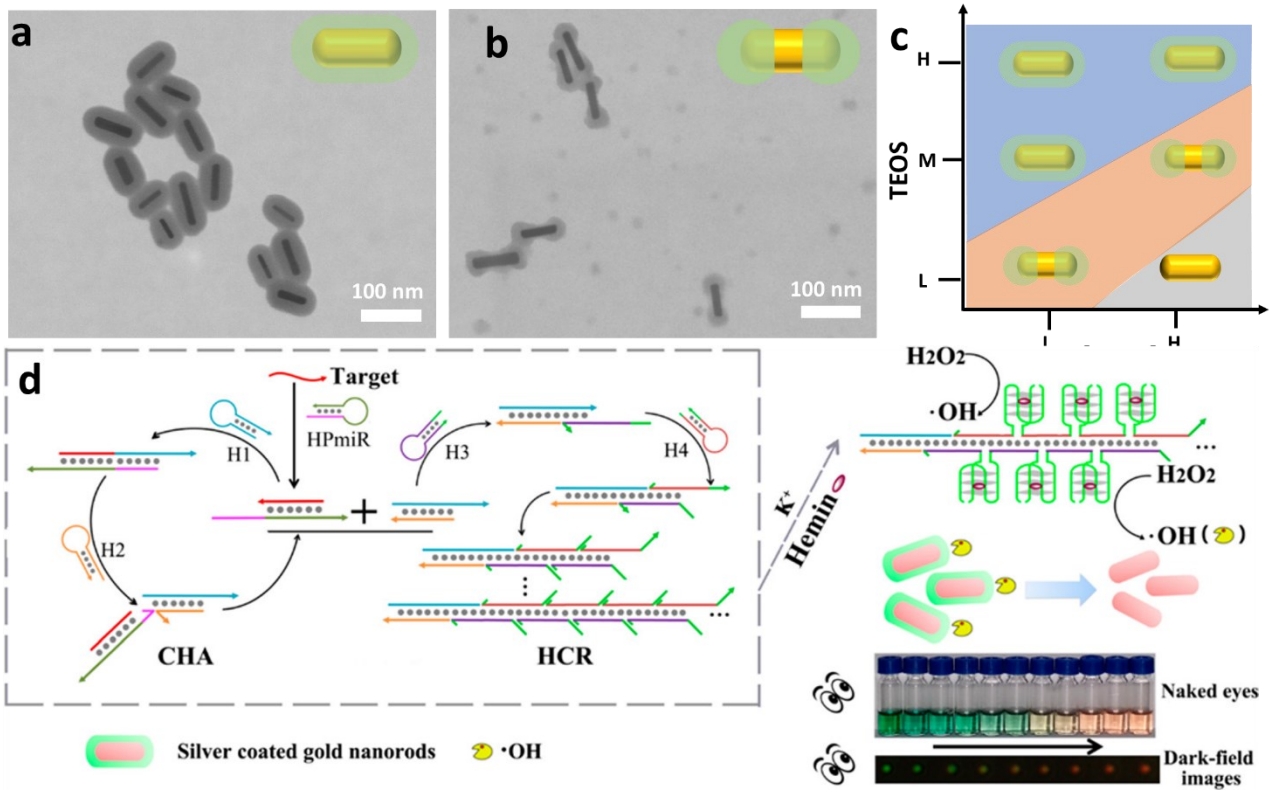

Figure 3: TEM images of AuNR@SiO_2 obtained at constant TEOS concentration and with (a) 1 mM CTAB and (b) 9 mM CTAB. (c) Shape of the silica coating under various conditions.[55] (d) The illustration of the Principle for Determination of miR-141.[66] Reprinted with permission from ref. 55 and 66. Copyright 2019 and 2017, American Chemical Society.

Hydroxyl radicals are one of the strongest oxidants which could etch the silver on the surface of the AuNR and result in a notable SPR shift which is visibly accompanied by an obvious colour change. The detection limit was down to 50 aM, indicating that the proposed strategy has ultrahigh sensitivity.[66] Wang and co-workers used cetyltrimethylammonium chloride (CTAC) surfactant to control the silver shell formation on the AuNRs, resulting in highly uniform shape and size.[62] They also provided a systematic study on the plasmon resonances of silver coated

AuNRs of varying thickness which is useful for applying this material in various plasmon-enhanced spectroscopies.

Using seed-mediated growth, Wang and co-workers have a detailed study on the effect of surface capping agents (CTAC or CTAB), ascorbic acid reduction capability, reaction temperature, and structure-directing foreign ions, such as Ag^+, on the formation of Pd nanoshells over the surface of AuNRs with finely controlled dimensions and architectures.[64] While Pd and Pt have been less studied in sensing applications due to their broader and weaker LSPR band, it has been reported that Pd or Pt coated AuNRs exhibit greater refractive index sensitivity than the uncoated AuNRs with similar plasmon wavelengths.[67-69]

Coating AuNRs with magnetic metals is another approach to produce additional functionality for the sensing process. [70-71] For example, Zhang et al. demonstrated the synthesis of Fe_3O_4-AuNR nanocomposites through a seed-mediated growth method and used these nanocomposites as a substrate in the SPR biosensor to detect goat IgM. The magnetic property of this nanocomposite enabled easy immobilization by an external magnet which can be beneficial for biosensors.[70]

2.3.3 Surface modification with Graphene

Graphene is a 2-dimensional carbon allotrope with atomic thickness that exhibits unique electrical, optical, mechanical and thermal properties.[72] Such features allow graphene and its derivatives, such as graphene oxide (GO) and reduced graphene oxide (rGO), to be widely used in sensors. To enhance the performance of sensors, researchers often integrate them with other inorganic nanomaterials including metal nanoparticles as has been discussed in several high-quality review articles.[73-76]

In recent years, surface modification of AuNRs with graphene and its derivatives has become popular for improved sensing performance, which is most commonly achieved via electrostatic assembly strategy. For example, Hu et al. prepared GO-AuNR hybrid composites by the electrostatic assembly method.[77] In their work, poly (N-vinyl-2-pyrrolidine) (PVP) was first introduced into the negative charged GO dispersion, where PVP acts as a stabilizing surfactant to increase the stability of GO dispersion and protect GO from aggregation with the addition of positive CTAB-capped AuNRs. The resulting GO-AuNRs hybrid composites show potential as substrates for enhancing Raman signals of adsorbed molecules. Other graphene/AuNRs hybrid composites are also commonly prepared via in-situ growing AuNRs on the surface of graphene[78-80] and chemical vapor deposition[81] before further applications.

Techniques for using surface modified AuNRs on sensing applications.

Although surface modification allows the sensing performance of AuNRs to be improved, as discussed earlier, the interesting LSPR properties of AuNRs are the essential component to allow important sensing and detecting applications to be possible. As noted in the introduction section, the LSPR properties vary enormously depending on morphology, material composition, the surrounding environment, as well as interactions between the AuNRs. Thus, based on the needs of the desired application, there are few classes of techniques that have been developed for sensing and detection of various analytes such as heavy metal ions, toxins, biomolecules, and tumor or cancer biomarkers. In this section, we will summarize and discuss the recent published work on the specific techniques related with using surface modified AuNRs for sensing. It is worthy to mention that although this section describes a good number of sensing techniques, there are other sensing techniques using surface modified AuNRs which will not be covered in this article such as fluorescence-involved sensing,[82-83] chirality sensing,[84-85] electrochemical sensing,[86-88] etc..

3.1. Colourimetric sensing via shape change and aggregation

Colourimetric sensing, monitoring the colour change of the sensor when they encounter analytes of interest, is a classic approach to optical sensing. Such an approach is popular due to its low cost, high accessibility and sensitivity. AuNR based colorimetric sensing mainly relies on either morphology changes which can be achieved by either (1) inducing etching or growth of nanostructures,[89-95] or (2) the aggregation state of AuNR based system which can be induced by either reducing the stability of nanoparticles through the manipulation of electrostatic forces, or by using the crosslinking mechanism (i.e. using specific recognition elements) to form bridging between AuNRs. The resulting colour-change behaviour can be monitored either by benchtop UV-Vis spectrophotometers or potentially even by simply naked eye readout. **Table I** shows some typical examples for colourimetric sensing with surface modified AuNRs during the past decade. Additionally, Ghourchian and coworkers have recently provided an excellent review of the colorimetric sensing using AuNRs.[96]

The use of colourimetric sensing systems to detect mercury via surface modification of AuNRs can be achieved by either strategy (etching/growth or aggregation) or both. For example, Zhao and co-workers developed a sensing method by combining the etching and aggregation effect. In their work, AuNRs were modified with silver shells whose surface was linked with cysteine ligands and the resulting nanostructures were used for Hg(II) detection. The cysteine ligands on the surface interacted with Hg(II) at a low concentration (under 60 μM) and induced aggregation of silver coated AuNRs, which causes LSPR to decrease rapidly. Whereas when the Hg(II) was at a high concentration (greater than 60 μM), the adherent cysteine molecules broke away from the surface due to the intense Hg-S bond and the bare nanorods were etched under the action of Hg(II).[97]

Mercury(II) does not interact with AuNRs themselves, but reduction to metallic mercury(0) with sodium borohydride leads to the formation of a gold-mercury amalgam which appears to change the morphology of the AuNRs.[24, 98] Our group used PEG-thiol-modified AuNRs to detect mercury via amalgamation. In our system, mercury(II) can first form Hg-S bonds with thiol ligands, removing them from the surface of AuNRs, resulting in bare AuNRs to interact with mercury after its reduction. By adjusting the extent of Hg-S bond formation, the total number of PEG-thiol on the surface of AuNRs in the sensing system can be controlled, which allows an adjustable

peak plasmonic response region and impacts the plasmonic responses of the system to the same concentration of mercury.[24] When sensing for the presence of toxins, biomolecules, as well as tumor or cancer biomarkers using AuNRs, these are mostly detected based on the aggregation approach where the assembly of surface conjugated AuNRs occurs via interactions with polymers, antibody–antigen reaction, biotin–strepavidin connectors and DNA. Due to the anisotropic structure of AuNRs, the ligands' modification can be selective on the surface either on tip or side which will cause different types of assembly. For example, Zhang et al. used helper DNA to conjugate and block the tip of AuNRs, so then the ademosine aptamers were attached to the sides of AuNRs. As shown in Scheme 2, when the helper DNA was introduced with certain concentration, it would take priority to occupy both ends of AuNRs since the ends have less absorbed CTAB and are thus more accessible for DNA to anchor on through the Au-S bond. When adenosine aptamers (C1 and C2) were added in solution, they were then immobilized at the sides of AuNRs. In the presence of adenosine, the C1- and C2- modified AuNRs side by side self-assembled to form a sandwich structure by specifically capturing the target adenosine, leading to the decrease in intensity and blue shift of absorption peak and change of the solution's colour. [99]

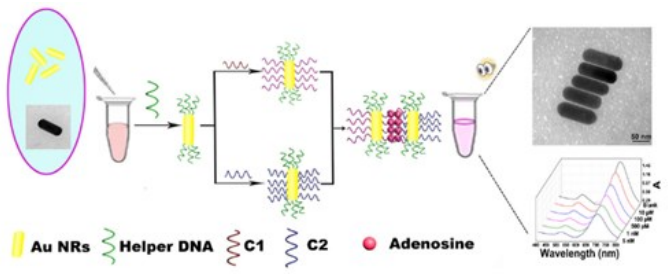

Scheme 2 Schematic of the colorimetric adenosine assay based on the side-by-side self-assembly.[99] Reprinted with permission from ref. 99. Copyright 2019, Springer.

3.2.Sensing based on refractive index change

Binding analytes to the surface of AuNRs will change their local dielectric environment, which then leads to significant shifts of the longitudinal absorption band of AuNRs. This refractive index (RI) change-induced LSPR shift has been used widely as a read-out method for chemical and biomedical sensors. Due to the anisotropic geometry of AuNRs, the electric field associated with the surface plasmon resonance is largest at the tip of AuNRs and decreases gradually along the sides. In addition, such electrical field enhancement decays exponentially with the distance from the surface of AuNRs.[42] Thus, for optimal RI sensing, the analyte should ideally be placed in close proximity to the tip of the AuNRs.

To facilitate this, surface modification allows improved sensitivity and selectivity by functionalizing the surface (particularly, in this case, the tips) of the AuNRs with a specific functional group that will preconcentrate the target analytes and produce an effective adsorption of those analytes on the surface of AuNRs. Although there are some reports on using sensing based on RI changes to detect metal ions,[100] using RI changes for biosensing is much more pervasive.

Antibodies and aptamers are the most commonly used bioreceptors for RI-based biosensors using AuNRs.[101-103] Zijlstra and coworkers surface modified a single AuNR at the tip of the particle with biotin, which can bind to the protein of interest and this binding event was detected by monitoring its LSPR due to the IR change.[104] By combining nanorods with distinct LSPR wavelengths, a multiplex AuNR-based sensor can be developed.[105-106] Tang and co-workers synthesized AuNRs with various aspect ratios which were immobilized by antibodies for cardiac troponin I and myoglobin to develop a multiplexed GNR nanosensor to simultaneously detect both cardiac biomarkers at various concentrations.[105] Their study shows the first demonstration of the multiplex nanorod based biosensor application for these two clinically relevant cardiac biomarkers. Surface modifying AuNRs with natural biotin for capture of target biomolecules is ubiquitous in the applications of disease diagnosis, toxicology testing and biotechnology. However, natural antibodies suffer from numerous shortcomings such as poor chemical stability, excessive cost and limited shelf-life.

Surface modifying AuNRs with artificial biotin by molecular imprinting for detecting target biomarkers is a way to overcome those drawbacks.[107-108] Abbas at el. demonstrated a strategy for imprinting biomolecule on the surface of AuNRs. First, the AuNRs with CTAB surfactant will be adsorbed on a glass substrate. The protein template (the analyte of interest) will be immobilized on the surface of AuNRs (particularly on the tip, if the concentration is limited) by using a mixture of p-aminothiophenol (p-ATP) and glutaraldehyde (GA). In aqueous solution, p-ATP binds spontaneously to the gold surface with its thiol group (priority on the tip of the AuNR due to the accessibility). Then, GA molecules form oligomers of variable sizes with a free aldehyde group at each end of the molecules (Figure 4a). As a result, GA plays a role of a crosslinker to bind protein templates with p-ATP molecules. Following the immobilization of the template, organo-siloxane monomers trimethoxypropylsilane (TMPS) and (3-aminopropyl)trimethoxysilane (APTMS), which are hydrolytically unstable, are copolymerized onto the surface of the modified AuNRs (Figure 4b). The subsequent condensation of the transient silanol groups yields an aminopropyl-functional amorphous polymer and entrapment of the protein templates. Finally, the templates are removed by breaking the imine bonds of the cross-linker using a mixture of sodium dodecyl sulfate and oxalic acid. The formed cavities could then be used to trap the protein of interest.

The localized plasmonic property of the AuNRs enables monitoring, not only of the process during each step, but also of direct detection of protein capture and release. Figure 4c shows the LSPR wavelength shift following different steps of the imprinting process with two types of biomolecules. The accumulated shift due to the imprinting process is ≈16 nm. The removal of protein induces a blue-shift (step 5, in the Figure 4 c). Repeated cycles of protein capture and release show strong stability of the imprinted AuNR surface and demonstrate

excellent reproducibility for the protein used. Such artificial antibody modifications on the surface of AuNRs opens up a novel class of plasmonic nanostructures with built-in biorecognition capability.[107]

Table 1: Examples of colourimetric sensing with surface modified AuNRs during the past decade.

Analyte	Surface modification	Sensing strategy	Detection limit	reference
Hg^{2+}	Cysteine modified silver coated AuNRs	Cysteine modification causes the aggregation of silver coated AuNR s at its low conc. (<60 µM) while silver shell was etched away by the action of Hg^{2+} at its high conc. (>60 µM).	Low conc. range: 0.273 µM; High conc. range: 1.065 µM	97
	1-[2-(octylamino)ethyl]-3,5-diphenylpyrazole (PyL) modified AuNRs	PyL has high affinity to Hg^{2+}. In the present Hg2+, PyL modified AuNR form end to end assembly induced by Hg^{2+}.	3 ppt	109
Hg^{0}	PEG-thiol modified AuNRs	Hg^{2+} first forms Hg-S bond with thiol ligands and removes them from the surface of AuNRs which result in bare AuNRs to form amalgamation with Hg^{0}.	From 20-90 µg/L based on various amount of PEG-thiol on AuNRs surface.	24
Cu^{2+}	AuNR surface adsorbed with thiosulfate ($S_2O_3^{2-}$) and ammonia (NH_3)	Cu^{2+} and NH_3 form $Cu(NH_3)_4^{+}$ which acts as an oxidant and can etch AuNRs under $S_2O_3^{2-}$. Such morphological changes decreases the absorbance peak of the AuNR solution.	1.6 nM	110
Al^{3+}	Tannic acid coated AuNR	Tannic acid prefers to form complexation and binding to Al^{3+} which induces side to side assembly of AuNRs	0.09 µM	111,
Pb^{2+}	Cysteine modified AuNR	In the present Pb^{2+}, cysteine modified AuNRs form side to side assembly of AuNRs.	0.1 nM	112
	Thiosulfate modified AuNR	In the thiosulphate system, the additional Pb^{2+} leads the formation of AuPb2 and AuPb3 alloys on the gold surface which results in morphology change of AuNR to nanosphere.	0.1 µM	113
As^{3+}	Dithiothreitol (DDT) modified AuNR	The As(III) ions can bind with three DTT-AuNRs through an As-S linkage and induce the aggregation of DTT-AuNRs	38 nM	114
As (III & V)	AuNRs modified with poly(ethylene glycol) methyl ether thiol (mPEG-SH) and meso-2,3-dimercaptosuccinic acid (DMSA).	When As^{III} and As^{V} ions are added to GNR-PEG-DMSA solution, the ions will induce assembly of nanorod particles and as a result, the colour solution of AuNRs changes markedly from dark bluish purple to almost colourless.	1 ppb	26
Cr^{6+}	Bovine serum albumin (BSA) modified AuNR	Acid-digested Cr^{6+} can etch BSA coated AuNRs which reduces their aspect ratio and can be monitored by UV-Vis； BSA modification provides stability and less environmental toxicity.	0.32 µM	115
Aflatoxin B1 (AFB1)	AFB1-BSA modified AuNRs	Based on antibody-antigen interaction, the modified AuNR, the existence of AFB1 molecules prevented aggregation of modified AuNRs.	0.16 ng/mL	116
BPO	Silver shell deposited Au NR	In the presence of BPO, Ag shells are oxidized to Ag^{+} and etched in a way which causes the longitudinal LSPR peak red-shifting as well as a sharp-contrast multicolour change.		90
Ochratoxin A (OTA)	Thiol-modified DNA decorated on the sides of AuNRs	In the present OTA, the AuNRs dispersed because of specific aptamer–OTA recognition and conformational changes in the aptamer. In the absence of OTA, AuNRs assembled side-by-side through DNA hybridization.	0.22 ng mL^{-1}	117
Adenosine	Helper DNA to occupy the ends of AuNR and adenosine aptamers attach to the side of AuNR	Aptamer induced side-by-side assembly.	3.3 pM	99
Hepatitis A virus Vall7 polyprotein gene (HVA)	DNA modified AuNRs	Due to DNA interaction, the captured DNA will pair with HVA which causes assembly of AuNRs. Using additional helper DNA can control the side to side or tip to tip assembly.	Side-by-side assembly: 0.05 pM	118

3.3.Sensing based on SERS

AuNRs enhance the inelastic light scattering of molecular vibrations near metal surfaces, which allow them to be used as optical sensors for SERS-based detection. The high EM field enhancement observed at the tips of the NRs and at the junction of NR assemblies has been used to increase the SERS signal enhancement, which in turn boosts the sensitivity of SERSs based sensing platforms.

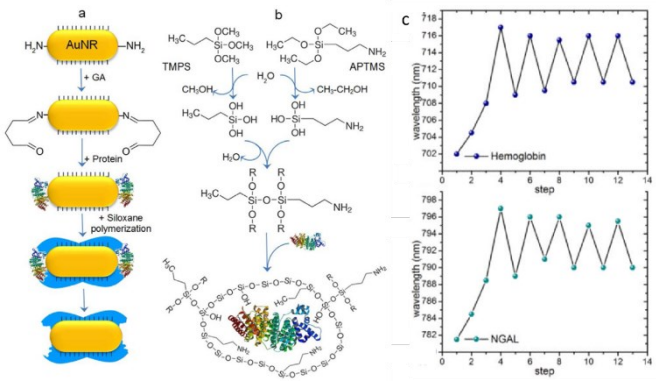

Figure 4: Concept and mechanism of plasmonic hot spot-localized imprinting of AuNRs. a) Surface chemistry of the molecular imprinting process involving the preferential attachment of p-ATP to the ends of the AuNR, followed by glutaraldehyde (GA) interaction with the primary amine groups of p-ATP on one side and with the amine functions of the protein on the other side. Finally, siloxane monomers are polymerized in the presence of the protein templates. The release of the protein results in a polymeric recognition cavity (in blue). b) Co-polymerization reaction of the organo-siloxane monomers APTMS and TMPS. In aqueous environment, the monomers undergo hydrolysis then condensation to yield amorphous siloxane copolymer. c) Shift of the LSPR wavelength following the different steps of the imprinting process. Each measurement point represents the shift obtained at the end of each step indicated with numbers. Steps 1 to 4 correspnond to AuNR, AuNR-pATP/GA, AuNR-pATP/GA-protein and AuNR-pATP/GA-protein-siloxane copolymer, respectively. Steps 5 to 13 correspond to 4 cycles of protein capture and release, resulting in a red-shift or blue-shift, respectively.[107] Reprinted with permission from ref. 107. Copyright 2013, Wiley.

Surface modification is a commonly used approach to enhance the Raman signal. As discussed previously, one strategy is to surface functionalize AuNRs with certain surfaces that can effectively attract and capture analyte molecules from the solution which results in enhanced Raman signals. Charge attractions, antibody-antigen interactions, molecule size selection functions created by silica, or the use of metal-organic frameworks (MOF) have all been exploited in this regard.[119] For example, as mentioned above, Singamameni group has used the LbL method to modify the AuNRs with negative and positive charges on the surface which then can effectively capture their opposite charged analytes. Due to the diverse chemical functionalizations of AuNRs, the different responses of Raman spectra was collected, which allowed them to not only recognize the components of mixture but also quantify the mixing ratio.[35] Osterrieth and others reported the controlled encapsulation of AuNRs by Zr-MOF with a specific type of topology via a room-temperature MOF assembly. The MOF particle size can be controlled via the concentration of AuNRs, which can be used for selecting molecule species for diffusion inside the particle for AuNR- based SERS detection.[119]

Another strategy is to provide many "hot spots" on AuNRs via surface modification for large local EM field enhancement, which can produce a strong SERS signal. Various structures such as core-shell structure,[120-123] core-satellite structure,[124-125] or bulk assembled substrate[126] can be created via surface modification for SERS applications. For example, Khlebtsov et al. immobilized Raman reporters between the surface of AuNRs and their silver shells. Their study shows that the molecules in the interior between gold and silver showed strong and uniform Raman intensity at least an order of magnitude higher than that of the molecules on the nanoparticle surface.[123] Shang et al. presented a SERS-active gold nanostructure with built-in EM hotspots formed by densely packed gold nanospheres on a AuNR surface.[125] As illustrated in Figure 5a, thiolated DNA was first conjugated to AuNRs. The Raman reporter (Cy3) labelled DNA strand 2 was anchored to the rod surface via hybridization with the DNA strand 1. Gold nanospheres were then densely synthesized around the AuNRs forming the core-satellite structure, which they call a "bumpy nanostructure". This approach allows for positioning of the Raman reporters (Cy3) within the locally enhanced EM field and reduced the possibility of detachment or diffusion of the Cy3 as well as signal fluctuation.

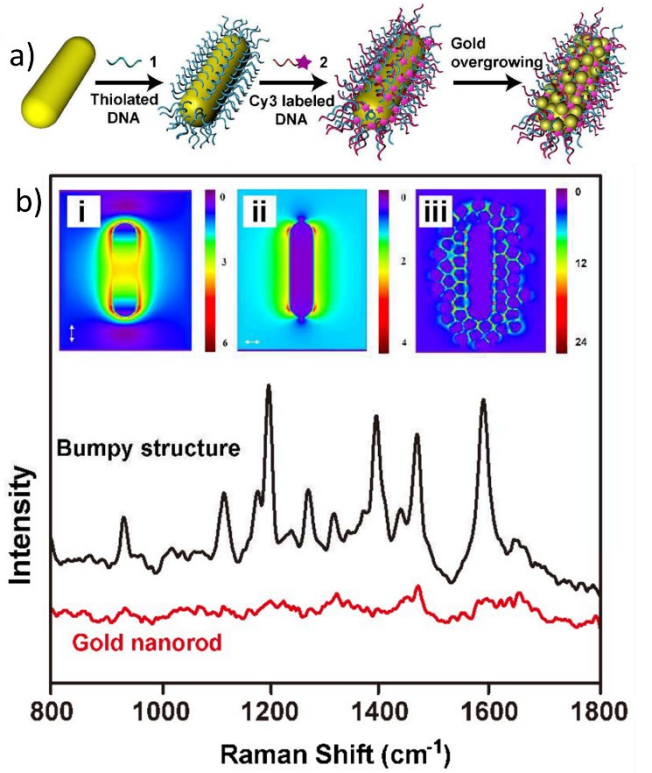

Figure 5 a) Schematic illustration of the synthesis of SERS active gold nanostructure by modifying AuNR with a Raman dye-labelled DNA, and subsequent growth of the small gold nanoparticles on the AuNR. b) SERS spectra from the nanorod core and the bumpy nanostructure solutions, showing significantly enhanced SERS activity of the bumpy nanostructures, compared to the AuNR. The inset images show electromagnetic field distribution around a AuNR (i) transverse plasmon, (ii) longitudinal plasmon) and (iii) a single bumpy nanostructure obtained using finite difference time domain (FDTD) simulations (incident light wavelength = 633nm), confirming the electromagnetic hotspots of the plasmonic nanostructures.[125] Reprinted with permission from ref. 125. Copyright 2018, Royal Society of Chemistry.

Finite-difference-time-domain (FDTD) simulations further confirmed the particle-to-particles and particles-to-nanorod plasmonic coupling and high-densitity distribution of EM hotspots in this case (Figure 5 inserts). SERS spectra from the nanostructure solutions showed significantly enhanced signals of Cy3 compared to that of AuNRs (Figure 5b). The analytical enhancement factor was calculated to be 1.56×10^4, 2 orders of magnitude higher than that from AuNR solution.[125]

Conclusions and outlook

Surface modification of AuNRs is a necessary path to effectively utilize the properties of AuNRs for sensing applications. In this review, we have focused on demonstrating the recent advances on surface functionalization of AuNRs and their use for improved sensing performance through various techniques. Significant progress has been made during the past decade on these topics. Surface modification methods include ligand exchange with the assistance of thiol-group, layer by layer assembly method, as well as depositing inorganic materials with desired surface and morphology. With the appropriated surface modification, the techniques that can be used for using those functionalized AuNRs are also summarized.

In the future, we believe that more research efforts should be focused on, but not limited to, the following directions: 1) Further improve and develop effective approaches on surface modification of functional ligand on AuNR, especially biomolecule related ligands; 2) Continue to find and refine methods to fabricate AuNRs/inorganic material hybrids with designed location/geometry and effective surface functions; 3) Better design sensing strategy by taking advantage of the surface manipulation methods. All these approaches could continue to open up additional opportunities for utilizing the special properties of AuNRs for improved sensing in a wide variety of applications. In addition, it is worthy to point out that the current characterization for surface modification is mostly focused on qualitative analysis which is no longer sufficient for further technological development. In the near future, the surface modification on the AuNRs should be evaluated by quantitative characterization protocols as well as possible models via theoretical calculations for clearer understanding than currently available. The directly in-situ study on the surface modification on the AuNRs could also be an exciting and emerging area to accurate analysis the environment of AuNRs surface.

Conflicts of interest

There are no conflicts to declare.

Acknowledgements

The authors would like to thank support from the National Science Foundation (grant no. 2108842).

Notes and references

1. Daniel, M.-C.; Astruc, D., Gold Nanoparticles: Assembly, Supramolecular Chemistry, Quantum-Size-Related Properties, and Applications toward Biology, Catalysis, and Nanotechnology. *Chem. Rev.* **2004,** *104* (1), 293-346.
2. Jain, P. K.; Huang, X.; El-Sayed, I. H.; El-Sayed, M. A., Noble Metals on the Nanoscale: Optical and Photothermal Properties and Some Applications in Imaging, Sensing, Biology, and Medicine. *Acc. Chem. Res.* **2008,** *41* (12), 1578-86.
3. Murphy, C. J.; Gole, A. M.; Hunyadi, S. E.; Stone, J. W.; Sisco, P. N.; Alkilany, A.; Kinard, B. E.; Hankins, P., Chemical sensing and imaging with metallic nanorods. *Chem. Commun.* **2008,** (5), 544-57.
4. Mayer, K. M.; Hafner, J. H., Localized Surface Plasmon Resonance Sensors. *Chem. Rev.* **2011,** *111* (6), 3828-57.
5. Link, S.; El-Sayed, M. A., Size and Temperature Dependence of the Plasmon Absorption of Colloidal Gold Nanoparticles. *J. Phys. Chem. B* **1999,** *103* (21), 4212-17.
6. Bao, Y.; Vigderman, L.; Zubarev, E. R.; Jiang, C., Robust Multilayer Thin Films Containing Cationic Thiol-Functionalized Gold Nanorods for Tunable Plasmonic Properties. *Langmuir* **2012,** *28* (1), 923-30.
7. Taylor, M. L.; Wilson, R. E.; Amrhein, K. D.; Huang, X., Gold Nanorod-Assisted Photothermal Therapy and Improvement Strategies. *Bioengineering* **2022,** *9* (5), 200.
8. Gans, R., Über die Form ultramikroskopischer Silberteilchen. *Annalen der Physik* **1915,** *352* (10), 270-84.
9. Das, R. S.; Agrawal, Y. K., Raman spectroscopy: Recent advancements, techniques and applications. *Vib. Spectrosc* **2011,** *57* (2), 163-76.
10. Campion, A.; Kambhampati, P., Surface-enhanced Raman scattering. *Chem. Soc. Rev.* **1998,** *27* (4), 241-50.
11. Scarabelli, L.; Sánchez-Iglesias, A.; Pérez-Juste, J.; Liz-Marzán, L. M., A "Tips and Tricks" Practical Guide to the Synthesis of Gold Nanorods. *J. Phys. Chem. Lett* **2015,** *6* (21), 4270-79.
12. Park, K.; Drummy, L. F.; Wadams, R. C.; Koerner, H.; Nepal, D.; Fabris, L.; Vaia, R. A., Growth Mechanism of Gold Nanorods. *Chem. Mater.* **2013,** *25* (4), 555-63.
13. Lohse, S. E.; Murphy, C. J., The Quest for Shape Control: A History of Gold Nanorod Synthesis. *Chem. Mater.* **2013,** *25* (8), 1250-61.
14. Zhang, Q.; Han, L.; Jing, H.; Blom, D. A.; Lin, Y.; Xin, H. L.; Wang, H., Facet Control of Gold Nanorods. *ACS Nano* **2016,** *10* (2), 2960-74.
15. Gole, A.; Murphy, C. J., Polyelectrolyte-Coated Gold Nanorods: Synthesis, Characterization and Immobilization. *Chem. Mater.* **2005,** *17* (6), 1325-30.
16. Wijaya, A.; Hamad-Schifferli, K., Ligand Customization and DNA Functionalization of Gold Nanorods via Round-Trip Phase Transfer Ligand Exchange. *Langmuir* **2008,** *24* (18), 9966-69.
17. Gorelikov, I.; Matsuura, N., Single-Step Coating of Mesoporous Silica on Cetyltrimethyl Ammonium Bromide-Capped Nanoparticles. *Nano Lett.* **2008,** *8* (1), 369-73.
18. Locatelli, E.; Ori, G.; Fournelle, M.; Lemor, R.; Montorsi, M.; Comes Franchini, M., Click Chemistry for the Assembly of Gold Nanorods and Silver Nanoparticles. *Chem. Eur. J.* **2011,** *17* (33), 9052-56.
19. Zhang, Z.; Lin, M., Fast loading of PEG–SH on CTAB-protected gold nanorods. *RSC Advances* **2014,** *4* (34), 17760-67.
20. Li, J.; Zhu, B.; Zhu, Z.; Zhang, Y.; Yao, X.; Tu, S.; Liu, R.; Jia, S.; Yang, C. J., Simple and Rapid Functionalization of Gold Nanorods with Oligonucleotides Using an mPEG-SH/Tween 20-Assisted Approach. *Langmuir* **2015,** *31* (28), 7869-76.
21. Liu, K.; Zheng, Y.; Lu, X.; Thai, T.; Lee, N. A.; Bach, U.; Gooding, J. J., Biocompatible Gold Nanorods: One-Step Surface Functionalization, Highly Colloidal Stability, and Low Cytotoxicity. *Langmuir* **2015,** *31* (17), 4973-80.
22. Cho, E. C.; Choi, S.-W.; Camargo, P. H. C.; Xia, Y., Thiol-Induced Assembly of Au Nanoparticles into Chainlike Structures and Their Fixing by Encapsulation in Silica Shells or Gelatin Microspheres. *Langmuir* **2010,** *26* (12), 10005-12.
23. Casas, J.; Venkataramasubramani, M.; Wang, Y. Y.; Tang, L., Replacement of cetyltrimethylammoniumbromide bilayer on gold nanorod by alkanethiol crosslinker for enhanced plasmon resonance sensitivity. *Biosens. Bioelectron.* **2013,** *49*, 525-30.

24. Crockett, J. R.; Win-Piazza, H.; Doebler, J. E.; Luan, T.; Bao, Y., Plasmonic Detection of Mercury via Amalgamation on Gold Nanorods Coated with PEG-Thiol. *ACS Appl. Nano Mater.* **2021,** *4* (2), 1654-63.
25. Yasun, E.; Gulbakan, B.; Ocsoy, I.; Yuan, Q.; Shukoor, M. I.; Li, C.; Tan, W., Enrichment and Detection of Rare Proteins with Aptamer-Conjugated Gold Nanorods. *Anal. Chem.* **2012,** *84* (14), 6008-15.
26. Priyadarshni, N.; Nath, P.; Nagahanumaiah; Chanda, N., DMSA-Functionalized Gold Nanorod on Paper for Colorimetric Detection and Estimation of Arsenic (III and V) Contamination in Groundwater. *ACS Sustain. Chem. Eng.* **2018,** *6* (5), 6264-72.
27. Requejo, K. I.; Liopo, A. V.; Zubarev, E. R., Gold Nanorod Synthesis with Small Thiolated Molecules. *Langmuir* **2020,** *36* (14), 3758-69.
28. He, J.; Unser, S.; Bruzas, I.; Cary, R.; Shi, Z.; Mehra, R.; Aron, K.; Sagle, L., The facile removal of CTAB from the surface of gold nanorods. *Colloids Surf. B* **2018,** *163*, 140-45.
29. Su, L.; Hu, S.; Zhang, L.; Wang, Z.; Gao, W.; Yuan, J.; Liu, M., A Fast and Efficient Replacement of CTAB with MUA on the Surface of Gold Nanorods Assisted by a Water-Immiscible Ionic Liquid. *Small* **2017,** *13* (11), 1602809.
30. Hamon, C.; Bizien, T.; Artzner, F.; Even-Hernandez, P.; Marchi, V., Replacement of CTAB with peptidic ligands at the surface of gold nanorods and their self-assembling properties. *J. Colloid Interface Sci.* **2014,** *424*, 90-97.
31. Matthews, J. R.; Payne, C. M.; Hafner, J. H., Analysis of Phospholipid Bilayers on Gold Nanorods by Plasmon Resonance Sensing and Surface-Enhanced Raman Scattering. *Langmuir* **2015,** *31* (36), 9893-900.
32. Chen, J.; Yan, J.; Sun, Q.; Zhu, W.; He, Z.; Pu, Y.; Li, L.; He, B., Cooling: A facile, rapid, reagent-free and DNA-saving method for functionalization of gold nanorods with thiolated DNA. *Mater. Lett.* **2022,** *308*, 131187.
33. Chen, H.; Chi, X.; Li, B.; Zhang, M.; Ma, Y.; Achilefu, S.; Gu, Y., Drug loaded multilayered gold nanorods for combined photothermal and chemotherapy. *Biomater. Sci.* **2014,** *2* (7), 996-1006.
34. Pastoriza-Santos, I.; Pérez-Juste, J.; Liz-Marzán, L. M., Silica-Coating and Hydrophobation of CTAB-Stabilized Gold Nanorods. *Chem. Mater.* **2006,** *18* (10), 2465-67.
35. Yilmaz, H.; Bae, S. H.; Cao, S.; Wang, Z.; Raman, B.; Singamaneni, S., Gold-Nanorod-Based Plasmonic Nose for Analysis of Chemical Mixtures. *ACS Appl. Nano Mater.* **2019,** *2* (6), 3897-905.
36. Tian, L.; Tadepalli, S.; Farrell, M. E.; Liu, K.-K.; Gandra, N.; Pellegrino, P. M.; Singamaneni, S., Multiplexed charge-selective surface enhanced Raman scattering based on plasmonic calligraphy. *J. Mater. Chem. C* **2014,** *2* (27), 5438-46.
37. Chen, J.; Jackson, A. A.; Rotello, V. M.; Nugen, S. R., Colorimetric Detection of Escherichia coli Based on the Enzyme-Induced Metallization of Gold Nanorods. *Small* **2016,** *12* (18), 2469-75.
38. Ni, W.; Yang, Z.; Chen, H.; Li, L.; Wang, J., Coupling between Molecular and Plasmonic Resonances in Freestanding Dye−Gold Nanorod Hybrid Nanostructures. *J. Am. Chem. Soc.* **2008,** *130* (21), 6692-93.
39. Gole, A.; Murphy, C. J., Biotin−Streptavidin-Induced Aggregation of Gold Nanorods: Tuning Rod−Rod Orientation. *Langmuir* **2005,** *21* (23), 10756-62.
40. Wang, J.; Dong, B.; Chen, B.; Jiang, Z.; Song, H., Selective photothermal therapy for breast cancer with targeting peptide modified gold nanorods. *Dalton Trans.* **2012,** *41* (36), 11134-44.
41. Urrutia, A.; Goicoechea, J.; Rivero, P. J.; Pildain, A.; Arregui, F. J., Optical fiber sensors based on gold nanorods embedded in polymeric thin films. *Sens. Actuators B: Chem.* **2018,** *255*, 2105-12.
42. Tian, L.; Chen, E.; Gandra, N.; Abbas, A.; Singamaneni, S., Gold Nanorods as Plasmonic Nanotransducers: Distance-Dependent Refractive Index Sensitivity. *Langmuir* **2012,** *28* (50), 17435-42.
43. Stöber, W.; Fink, A.; Bohn, E., Controlled growth of monodisperse silica spheres in the micron size range. *J. Colloid Interface Sci.* **1968,** *26* (1), 62-69.
44. Liz-Marzán, L. M.; Giersig, M.; Mulvaney, P., Synthesis of Nanosized Gold−Silica Core−Shell Particles. *Langmuir* **1996,** *12* (18), 4329-35.
45. Gao, Z.; Burrows, N. D.; Valley, N. A.; Schatz, G. C.; Murphy, C. J.; Haynes, C. L., In solution SERS sensing using mesoporous silica-coated gold nanorods. *Analyst* **2016,** *141* (17), 5088-95.
46. Meyer, S. M.; Murphy, C. J., Anisotropic silica coating on gold nanorods boosts their potential as SERS sensors. *Nanoscale* **2022,** *14* (13), 5214-26.
47. Kang, H.; Haynes, C., Interactions between Silica-Coated Gold Nanorod Substrates and Hydrophobic Analytes in Colloidal Surface-Enhanced Raman Spectroscopy. *J. Phys. Chem. C.* **2019,** *123* (40), 24685-97.
48. Wu, W.-C.; Tracy, J. B., Large-Scale Silica Overcoating of Gold Nanorods with Tunable Shell Thicknesses. *Chem. Mater.* **2015,** *27* (8), 2888-94.
49. Abadeer, N. S.; Brennan, M. R.; Wilson, W. L.; Murphy, C. J., Distance and Plasmon Wavelength Dependent Fluorescence of Molecules Bound to Silica-Coated Gold Nanorods. *ACS Nano* **2014,** *8* (8), 8392-406.
50. Yoon, S.; Lee, B.; Kim, C.; Lee, J. H., Controlled Heterogeneous Nucleation for Synthesis of Uniform Mesoporous Silica-Coated Gold Nanorods with Tailorable Rotational Diffusion and 1 nm-Scale Size Tunability. *Cryst. Growth Des* **2018,** *18* (8), 4731-36.
51. van der Hoeven, J. E. S.; Gurunarayanan, H.; Bransen, M.; de Winter, D. A. M.; de Jongh, P. E.; van Blaaderen, A., Silica-Coated Gold Nanorod Supraparticles: A Tunable Platform for Surface Enhanced Raman Spectroscopy. *Adv. Funct. Mater.* **2022,** *32* (27), 2200148.
52. Rowe, L. R.; Chapman, B. S.; Tracy, J. B., Understanding and Controlling the Morphology of Silica Shells on Gold Nanorods. *Chem. Mater.* **2018,** *30* (18), 6249-58.
53. Pellas, V.; Blanchard, J.; Guibert, C.; Krafft, J.-M.; Miche, A.; Salmain, M.; Boujday, S., Gold Nanorod Coating with Silica Shells Having Controlled Thickness and Oriented Porosity: Tailoring the Shells for Biosensing. *ACS Appl. Nano Mater.* **2021,** *4* (9), 9842-54.
54. Zhang, Y.; Qian, J.; Wang, D.; Wang, Y.; He, S., Multifunctional Gold Nanorods with Ultrahigh Stability and Tunability for In Vivo Fluorescence Imaging, SERS Detection, and Photodynamic Therapy. *Angew. Chem. Int. Ed.* **2013,** *52* (4), 1148-51.
55. Wang, M.; Hoff, A.; Doebler, J. E.; Emory, S. R.; Bao, Y., Dumbbell-Like Silica Coated Gold Nanorods and Their Plasmonic Properties. *Langmuir* **2019,** *35* (51), 16886-92.
56. Huang, C.-M.; Chung, M.-F.; Souris, J. S.; Lo, L.-W., Controlled epitaxial growth of mesoporous silica/gold nanorod nanolollipops and nanodumb-bells. *APL Materials* **2014,** *2* (11), 113312.
57. Wang, F.; Cheng, S.; Bao, Z.; Wang, J., Anisotropic Overgrowth of Metal Heterostructures Induced by a Site-Selective Silica Coating. *Angew. Chem. Int. Ed.* **2013,** *52* (39), 10344-48.
58. Khlebtsov, B. N.; Khanadeev, V. A.; Tsvetkov, M. Y.; Bagratashvili, V. N.; Khlebtsov, N. G., Surface-Enhanced Raman Scattering Substrates Based on Self-Assembled PEGylated Gold and Gold–Silver Core–Shell Nanorods. *J. Phys. Chem. C.* **2013,** *117* (44), 23162-71.
59. Nguyen, L.; Dass, M.; Ober, M. F.; Besteiro, L. V.; Wang, Z. M.; Nickel, B.; Govorov, A. O.; Liedl, T.; Heuer-Jungemann, A., Chiral Assembly of Gold–Silver Core–Shell Plasmonic Nanorods on DNA Origami with Strong Optical Activity. *ACS Nano* **2020,** *14* (6), 7454-61.

60. Zhang, W.; Goh, H. Y. J.; Firdoz, S.; Lu, X., Growth of Au@Ag Core–Shell Pentatwinned Nanorods: Tuning the End Facets. *Chem. Eur. J.* **2013,** *19* (38), 12732-38.
61. Becker, J.; Zins, I.; Jakab, A.; Khalavka, Y.; Schubert, O.; Sönnichsen, C., Plasmonic Focusing Reduces Ensemble Linewidth of Silver-Coated Gold Nanorods. *Nano Lett.* **2008,** *8* (6), 1719-23.
62. Jiang, R.; Chen, H.; Shao, L.; Li, Q.; Wang, J., Unraveling the Evolution and Nature of the Plasmons in (Au Core)–(Ag Shell) Nanorods. *Adv. Mater.* **2012,** *24* (35), OP200-OP07.
63. Su, G.; Jiang, H.; Zhu, H.; Lv, J.-J.; Yang, G.; Yan, B.; Zhu, J.-J., Controlled deposition of palladium nanodendrites on the tips of gold nanorods and their enhanced catalytic activity. *Nanoscale* **2017,** *9* (34), 12494-502.
64. Jing, H.; Wang, H., Controlled overgrowth of Pd on Au nanorods. *CrystEngComm* **2014,** *16* (40), 9469-77.
65. Khanal, B. P.; Zubarev, E. R., Polymer-Functionalized Platinum-On-Gold Bimetallic Nanorods. *Angew. Chem. Int. Ed.* **2009,** *48* (37), 6888-91.
66. Gu, Y.; Song, J.; Li, M.-X.; Zhang, T.-T.; Zhao, W.; Xu, J.-J.; Liu, M.; Chen, H.-Y., Ultrasensitive MicroRNA Assay via Surface Plasmon Resonance Responses of Au@Ag Nanorods Etching. *Anal. Chem.* **2017,** *89* (19), 10585-91.
67. Feng, L.; Wu, X.; Ren, L.; Xiang, Y.; He, W.; Zhang, K.; Zhou, W.; Xie, S., Well-Controlled Synthesis of Au@Pt Nanostructures by Gold-Nanorod-Seeded Growth. *Chem. Eur. J.* **2008,** *14* (31), 9764-71.
68. Zhang, K.; Xiang, Y.; Wu, X.; Feng, L.; He, W.; Liu, J.; Zhou, W.; Xie, S., Enhanced Optical Responses of Au@Pd Core/Shell Nanobars. *Langmuir* **2009,** *25* (2), 1162-68.
69. Lu, B.; Kan, C.; Ke, S.; Xu, H.; Ni, Y.; Wang, C.; Shi, D., Geometry-Dependent Surface Plasmonic Properties and Dielectric Sensitivity of Bimetallic Au@Pd Nanorods. *Plasmonics* **2017,** *12* (4), 1183-91.
70. Zhang, H.; Sun, Y.; Wang, J.; Zhang, J.; Zhang, H.; Zhou, H.; Song, D., Preparation and application of novel nanocomposites of magnetic-Au nanorod in SPR biosensor. *Biosens. Bioelectron.* **2012,** *34* (1), 137-43.
71. Zhang, H.; Sun, Y.; Gao, S.; Zhang, H.; Zhang, J.; Bai, Y.; Song, D., Studies of gold nanorod-iron oxide nanohybrids for immunoassay based on SPR biosensor. *Talanta* **2014,** *125*, 29-35.
72. Verma, D.; Goh, K. L., Chapter 11 - Functionalized Graphene-Based Nanocomposites for Energy Applications. In *Functionalized Graphene Nanocomposites and their Derivatives*, Jawaid, M.; Bouhfid, R.; Kacem Qaiss, A. e., Eds. Elsevier: 2019; pp 219-43.
73. Yildiz, G.; Bolton-Warberg, M.; Awaja, F., Graphene and graphene oxide for bio-sensing: General properties and the effects of graphene ripples. *Acta Biomaterialia* **2021,** *131*, 62-79.
74. Peña-Bahamonde, J.; Nguyen, H. N.; Fanourakis, S. K.; Rodrigues, D. F., Recent advances in graphene-based biosensor technology with applications in life sciences. *J. Nanobiotechnology* **2018,** *16* (1), 75.
75. Moldovan, O.; Iñiguez, B.; Deen, M. J.; Marsal, L. F., Graphene electronic sensors – review of recent developments and future challenges. *IET Circuits Devices Syst.* **2015,** *9* (6), 446-53.
76. Shahdeo, D.; Roberts, A.; Abbineni, N.; Gandhi, S., Chapter Eight - Graphene based sensors. In *Comprehensive Analytical Chemistry*, Hussain, C. M., Ed. Elsevier: 2020; Vol. 91, pp 175-99.
77. Hu, C.; Rong, J.; Cui, J.; Yang, Y.; Yang, L.; Wang, Y.; Liu, Y., Fabrication of a graphene oxide–gold nanorod hybrid material by electrostatic self-assembly for surface-enhanced Raman scattering. *Carbon* **2013,** *51*, 255-64.
78. Caires, A. J.; Alves, D. C. B.; Fantini, C.; Ferlauto, A. S.; Ladeira, L. O., One-pot in situ photochemical synthesis of graphene oxide/gold nanorod nanocomposites for surface-enhanced Raman spectroscopy. *RSC Adv.* **2015,** *5* (58), 46552-57.
79. Sun, B.; Wu, J.; Cui, S.; Zhu, H.; An, W.; Fu, Q.; Shao, C.; Yao, A.; Chen, B.; Shi, D., In situ synthesis of graphene oxide/gold nanorods theranostic hybrids for efficient tumor computed tomography imaging and photothermal therapy. *Nano Research* **2017,** *10* (1), 37-48.
80. Khan, M. S.; Pandey, S.; Bhaisare, M. L.; Gedda, G.; Talib, A.; Wu, H. F., Graphene oxide@gold nanorods for chemo-photothermal treatment and controlled release of doxorubicin in mice Tumor. *Colloids Surf. B* **2017,** *160*, 543-52.
81. Lai, X.-F.; Zou, Y.-X.; Wang, S.-S.; Zheng, M.-J.; Hu, X.-X.; Liang, H.; Xu, Y.-T.; Wang, X.-W.; Ding, D.; Chen, L.; Chen, Z.; Tan, W., Modulating the Morphology of Gold Graphitic Nanocapsules for Plasmon Resonance-Enhanced Multimodal Imaging. *Anal. Chem.* **2016,** *88* (10), 5385-91.
82. Lu, X.; Dong, X.; Zhang, K.; Han, X.; Fang, X.; Zhang, Y., A gold nanorods-based fluorescent biosensor for the detection of hepatitis B virus DNA based on fluorescence resonance energy transfer. *Analyst* **2013,** *138* (2), 642-50.
83. Hao, L.; Li, M.; Peng, K.; Ye, T.; Wu, X.; Yuan, M.; Cao, H.; Yin, F.; Gu, H.; Xu, F., Fluorescence Resonance Energy Transfer Aptasensor of Ochratoxin A Constructed Based on Gold Nanorods and DNA Tetrahedrons. *J. Agric. Food. Chem.* **2022,** *70* (34), 10662-68.
84. Wang, S.; Liu, X.; Mourdikoudis, S.; Chen, J.; Fu, W.; Sofer, Z.; Zhang, Y.; Zhang, S.; Zheng, G., Chiral Au Nanorods: Synthesis, Chirality Origin, and Applications. *ACS Nano* **2022,** *16* (12), 19789-809.
85. Wang, Y.; Zhou, X.; Xu, C.; Jin, Y.; Li, B., Gold Nanorods as Visual Sensing Platform for Chiral Recognition with Naked Eyes. *Sci. Rep.* **2018,** *8* (1), 5296.
86. Zhao, L.; Niu, G.; Gao, F.; Lu, K.; Sun, Z.; Li, H.; Stenzel, M.; Liu, C.; Jiang, Y., Gold Nanorods (AuNRs) and Zeolitic Imidazolate Framework-8 (ZIF-8) Core–Shell Nanostructure-Based Electrochemical Sensor for Detecting Neurotransmitters. *ACS Omega* **2021,** *6* (48), 33149-58.
87. Bai, W.; Huang, H.; Li, Y.; Zhang, H.; Liang, B.; Guo, R.; Du, L.; Zhang, Z., Direct preparation of well-dispersed graphene/gold nanorod composites and their application in electrochemical sensors for determination of ractopamine. *Electrochim. Acta* **2014,** *117*, 322-28.
88. Yang, S.; Cheng, Y.; Cheng, D.; Wang, Y.; Xu, H.; Li, M.; Jiang, T.; Wang, H., N-Doped Graphene-Supported Gold Nanorods for Electrochemical Sensing of Ascorbic Acid with Superior Sensitivity. *J. Electron. Mater.* **2023,** *52* (4), 2336-46.
89. Zhang, C.; Yin, A.-X.; Jiang, R.; Rong, J.; Dong, L.; Zhao, T.; Sun, L.-D.; Wang, J.; Chen, X.; Yan, C.-H., Time–Temperature Indicator for Perishable Products Based on Kinetically Programmable Ag Overgrowth on Au Nanorods. *ACS Nano* **2013,** *7* (5), 4561-68.
90. Lin, T.; Zhang, M.; Xu, F.; Wang, X.; Xu, Z.; Guo, L., Colorimetric detection of benzoyl peroxide based on the etching of silver nanoshells of Au@Ag nanorods. *Sens. Actuators B: Chem.* **2018,** *261*, 379-84.
91. Liu, W.; Hou, S.; Yan, J.; Zhang, H.; Ji, Y.; Wu, X., Quantification of proteins using enhanced etching of Ag coated Au nanorods by the Cu2+/bicinchoninic acid pair with improved sensitivity. *Nanoscale* **2016,** *8* (2), 780-84.
92. Wang, Y.; Zeng, Y.; Fu, W.; Zhang, P.; Li, L.; Ye, C.; Yu, L.; Zhu, X.; Zhao, S., Seed-mediated growth of Au@Ag core-shell nanorods for the detection of ellagic acid in whitening cosmetics. *Anal. Chim. Acta* **2018,** *1002*, 97-104.
93. Zhang, F.; Zhu, J.; Li, J.-J.; Zhao, J.-W., A promising direct visualization of an Au@Ag nanorod-based colorimetric sensor for

trace detection of alpha-fetoprotein. *J. Mater. Chem. C* **2015,** *3* (23), 6035-45.
94. Yang, R.; Song, D.; Wang, C.; Zhu, A.; Xiao, R.; Liu, J.; Long, F., Etching of unmodified Au@Ag nanorods: a tunable colorimetric visualization for the rapid and high selective detection of Hg2+. *RSC Adv.* **2015,** *5* (124), 102542-49.
95. Chen, L.; Li, R.; Yang, P., Plasmonic nanoprobes based on the shape transition of Au/Ag core–shell nanorods to dumbbells for sensitive Hg-ion detection. *RSC Adv.* **2019,** *9* (31), 17783-90.
96. Kermanshahian, K.; Yadegar, A.; Ghourchian, H., Gold nanorods etching as a powerful signaling process for plasmonic multicolorimetric chemo-/biosensors: Strategies and applications. *Coord. Chem. Rev.* **2021,** *442*, 213934.
97. Zhu, J.; Zhao, B.-z.; Qi, Y.; Li, J.-J.; Li, X.; Zhao, J.-W., Colorimetric determination of Hg(II) by combining the etching and aggregation effect of cysteine-modified Au-Ag core-shell nanorods. *Sens. Actuators B: Chem.* **2018,** *255*, 2927-35.
98. Kim, G. W.; Ha, J. W., Single-Particle Study on Hg Amalgamation Mechanism and Slow Inward Diffusion in Mesoporous Silica-Coated Gold Nanorods without Structural Deformation. *J. Phys. Chem. Lett* **2022,** *13* (11), 2607-13.
99. Zhang, X.; Kong, C.; Liu, Q.; Zuo, X.; Li, K.; Chen, Z., Colorimetric adenosine assay based on the self-assembly of aptamer-functionalized gold nanorods. *Microchim. Acta* **2019,** *186* (8), 587.
100. Hong, Y.; Jo, S.; Park, J.; Park, J.; Yang, J., High sensitive detection of copper II ions using D-penicillamine-coated gold nanorods based on localized surface plasmon resonance. *Nanotechnology* **2018,** *29* (21), 215501.
101. Chen, S.; Zhao, Q.; Zhang, L.; Wang, L.; Zeng, Y.; Huang, H., Combined detection of breast cancer biomarkers based on plasmonic sensor of gold nanorods. *Sens. Actuators B: Chem.* **2015,** *221*, 1391-97.
102. Liu, Y.; Wang, Y.; Yu, J.; Zhao, H.; Wang, M., Dual Ligands-Capped Gold Nanorod as a Localized Surface Plasmon Resonance Transducer for Label-Free Detection of O-GlcNAcylated Proteins. *J. Nanosci. Nanotechnol.* **2017,** *17* (1), 161-67.
103. Jo, S.; Lee, W.; Park, J.; Park, H.; Kim, M.; Kim, W.; Hong, J.; Park, J., Wide-range direct detection of 25-hydroxyvitamin D3 using polyethylene-glycol-free gold nanorod based on LSPR aptasensor. *Biosens. Bioelectron.* **2021,** *181*, 113118.
104. Zijlstra, P.; Paulo, P. M. R.; Orrit, M., Optical detection of single non-absorbing molecules using the surface plasmon resonance of a gold nanorod. *Nat. Nanotechnol.* **2012,** *7* (6), 379-82.
105. Tang, L.; Casas, J., Quantification of cardiac biomarkers using label-free and multiplexed gold nanorod bioprobes for myocardial infarction diagnosis. *Biosens. Bioelectron.* **2014,** *61*, 70-75.
106. Mei, Z.; Wang, Y.; Tang, L., Gold Nanorod Array Biochip for Label-Free, Multiplexed Biological Detection. *Methods Mol Biol* **2017,** *1571*, 129-41.
107. Abbas, A.; Tian, L.; Morrissey, J. J.; Kharasch, E. D.; Singamaneni, S., Hot Spot-Localized Artificial Antibodies for Label-Free Plasmonic Biosensing. *Adv. Funct. Mater.* **2013,** *23* (14), 1789-97.
108. Hu, R.; Luan, J.; Kharasch, E. D.; Singamaneni, S.; Morrissey, J. J., Aromatic Functionality of Target Proteins Influences Monomer Selection for Creating Artificial Antibodies on Plasmonic Biosensors. *ACS Appl. Mater. Interfaces* **2017,** *9* (1), 145-51.
109. Placido, T.; Aragay, G.; Pons, J.; Comparelli, R.; Curri, M. L.; Merkoçi, A., Ion-Directed Assembly of Gold Nanorods: A Strategy for Mercury Detection. *ACS Appl. Mater. Interfaces* **2013,** *5* (3), 1084-92.
110. Niu, X.; Xu, D.; Yang, Y.; He, Y., Ultrasensitive colorimetric detection of Cu2+ using gold nanorods. *Analyst* **2014,** *139* (11), 2691-94.
111. Park, J. H.; Seo, H. J.; Lu, P.; Moon, G. D.; Hyun, D. C., Tannic acid-coated gold nanorod as a spectrometric probe for sensitive and selective detection of Al3+ in aqueous system. *Journal of Industrial and Engineering Chemistry* **2021,** *94*, 507-14.
112. Cai, H.-H.; Lin, D.; Wang, J.; Yang, P.-H.; Cai, J., Controlled side-by-side assembly of gold nanorods: A strategy for lead detection. *Sens. Actuators B: Chem.* **2014,** *196*, 252-59.
113. Zhu, J.; Yu, Y.-Q.; Li, J.-J.; Zhao, J.-W., Colorimetric detection of lead(ii) ions based on accelerating surface etching of gold nanorods to nanospheres: the effect of sodium thiosulfate. *RSC Adv.* **2016,** *6* (30), 25611-19.
114. Ge, K.; Liu, J.; Fang, G.; Wang, P.; Zhang, D.; Wang, S., A Colorimetric Probe Based on Functionalized Gold Nanorods for Sensitive and Selective Detection of As(III) Ions. *Sensors* **2018,** *18* (7), 2372.
115. Alex, S. A.; Chandrasekaran, N.; Mukherjee, A., Using gold nanorod-based colorimetric sensor for determining chromium in biological samples. *J. Mol. Liq.* **2018,** *264*, 119-26.
116. Xu, X.; Liu, X.; Li, Y.; Ying, Y., A simple and rapid optical biosensor for detection of aflatoxin B1 based on competitive dispersion of gold nanorods. *Biosens. Bioelectron.* **2013,** *47*, 361-67.
117. Xu, X.; Xu, C.; Ying, Y., Aptasensor for the simple detection of ochratoxin A based on side-by-side assembly of gold nanorods. *RSC Adv.* **2016,** *6* (56), 50437-43.
118. Chang, L.; Khan, Y.; Li, L.; Yang, N.; Yin, P.; Guo, L., Colorimetric detection of HVA by self-assembly of Au nanorods with DNA double helices to give side-by-side and end-to-end structures. *RSC Adv.* **2017,** *7* (23), 13896-903.
119. Osterrieth, J. W. M.; Wright, D.; Noh, H.; Kung, C.-W.; Vulpe, D.; Li, A.; Park, J. E.; Van Duyne, R. P.; Moghadam, P. Z.; Baumberg, J. J.; Farha, O. K.; Fairen-Jimenez, D., Core–Shell Gold Nanorod@Zirconium-Based Metal–Organic Framework Composites as in Situ Size-Selective Raman Probes. *J. Am. Chem. Soc.* **2019,** *141* (9), 3893-900.
120. Wang, Y.; Wang, Y.; Wang, W.; Sun, K.; Chen, L., Reporter-Embedded SERS Tags from Gold Nanorod Seeds: Selective Immobilization of Reporter Molecules at the Tip of Nanorods. *ACS Appl. Mater. Interfaces* **2016,** *8* (41), 28105-15.
121. Liu, K.-K.; Tadepalli, S.; Tian, L.; Singamaneni, S., Size-Dependent Surface Enhanced Raman Scattering Activity of Plasmonic Nanorattles. *Chem. Mater.* **2015,** *27* (15), 5261-70.
122. Dai, L.; Song, L.; Huang, Y.; Zhang, L.; Lu, X.; Zhang, J.; Chen, T., Bimetallic Au/Ag Core–Shell Superstructures with Tunable Surface Plasmon Resonance in the Near-Infrared Region and High Performance Surface-Enhanced Raman Scattering. *Langmuir* **2017,** *33* (22), 5378-84.
123. Khlebtsov, B.; Khanadeev, V.; Khlebtsov, N., Surface-enhanced Raman scattering inside Au@Ag core/shell nanorods. *Nano Research* **2016,** *9* (8), 2303-18.
124. Kuttner, C.; Höller, R. P. M.; Quintanilla, M.; Schnepf, M. J.; Dulle, M.; Fery, A.; Liz-Marzán, L. M., SERS and plasmonic heating efficiency from anisotropic core/satellite superstructures. *Nanoscale* **2019,** *11* (38), 17655-63.
125. Shang, Y.; Shi, J.; Liu, H.; Liu, X.; Wang, Z.-G.; Ding, B., A bumpy gold nanostructure exhibiting DNA-engineered stimuli-responsive SERS signals. *Nanoscale* **2018,** *10* (20), 9455-59.
126. Mei, R.; Wang, Y.; Yu, Q.; Yin, Y.; Zhao, R.; Chen, L., Gold Nanorod Array-Bridged Internal-Standard SERS Tags: From

Ultrasensitivity to Multifunctionality. *ACS Appl. Mater. Interfaces* **2020,** *12* (2), 2059-66.

Table of Content/Abstract Graphics